Numerical simulation of wave packet evolution in a supersonic boundary layer

I.V. Egorov, A.V. Novikov, V.G.Soudakov and A.V. Fedorov***
**Central Aerohydrodynamic Institute named after prof. Zhukovsky (TsAGI)*
140180, Zhukovsky str. 1, Zhukovsky, Moscow region, Russia
***Moscow Institute of Physics and Technology*
140180, Gagarin str. 16, Zhukovsky, Moscow region, Russia

Abstract
Two-dimensional direct numerical simulation (DNS) of the wave-packet evolution in a supersonic boundary layer over a flat plate is carried out. At first a steady-state solution of supersonic flow over a flat plate at free-stream Mach number 6 is calculated. Then, unsteady disturbances (local in time) are induced in the free stream (fast or slow acoustic waves) or on the plate surface (local blowing-suction). Another case of a steady-state solution is a separated supersonic flow over a compression corner at the free-stream Mach number 5.373. Propagation of the wave packets through the separation point, recirculation zone and reattachment point is investigated.

1. Introduction

In quiet free streams on aerodynamically smooth surfaces, laminar-turbulent transition includes: 1) excitation of unstable normal modes by free-stream disturbances (fast and slow acoustic waves, vorticity and entropy perturbations) as well as by wall-induced disturbances (vibrations, periodic blowing-suction, surface irregularities, heating et al.); 2) downstream amplification of unstable disturbances that is described by linear stability theory (LST); 3) nonlinear breakdown to turbulence that occurs when the disturbance amplitudes achieve a certain critical level.[1,2] The first stage (receptivity) refers to mechanisms by which free-stream disturbances enter to the laminar boundary layer and generate unstable waves.[3]
Theoretical studies of Mack[4] and stability experiments[5-7] showed that the evolution of disturbances in supersonic boundary layers on a sharp cone and a flat plate is essentially different from the case of subsonic flows. Besides the first mode associated with Tollmien-Schlichting waves, there are the second and higher modes relevant to the family of trapped acoustic waves.[8,9] The second mode becomes a dominant instability at sufficiently high Mach numbers M (for the boundary layer on thermally insulated wall at zero pressure gradient, this occurs for M>4). In contrast to the first mode, the second-mode growth rate is maximal for two-dimensional (2-D) waves. This facilitates modelling of receptivity and instability phases associated with the second mode.
Fedorov and Khokhlov[10] developed a theoretical model of receptivity to acoustic disturbances radiating the sharp leading edge of a flat plate in supersonic flow. The boundary layer mode excited near the leading edge by fast acoustic wave can be referred as Mode F, and by slow acoustic wave – as Mode S. The theoretical predictions[11] of the receptivity coefficient agree well with the experimental data of Maslov et al.[12], which were obtained in the T-326 Mach 6 wind tunnel of the Institute of Theoretical and Applied Mechanics (ITAM, Novosibirsk). They are also consistent with the DNS.[13]
Unfortunately, experimental investigations of boundary-layer disturbances at hypersonic speeds are very limited. Numerical experiments seem to be the only way to acquire detailed data on the disturbance evolution in various phases of transition. This explains high interest in DNS of disturbances in boundary layers at supersonic and hypersonic speeds. Ma and Zhong[14-16] conducted a series of DNS related to receptivity and stability of high-speed flows over a parabolic leading edge and over a flat plate. Balakumar et al.[17-19] numerically investigated stability and receptivity of hypersonic boundary layer over a compression corner, blunted flat plate and cone. Egorov et al.[20-21] carried out series of numerical simulations of stability and receptivity of hypersonic boundary layer to the wall blowing-suction as well as to free-stream fast and slow acoustic waves with various angles of incidence. In these studies, a perturbation source run all the time and generates harmonic or time-periodic disturbances. However, natural sources induce wave-packets in a limited time interval rather than harmonic waves.

In the majority of theoretical and computational models, disturbances are treated as elementary waves of the discrete spectrum. In natural condition, disturbances of broad spectrum are typical. Their evolution occurs in both space and time and depends on flow properties and initial distribution. The first step in solving of this problem is to consider propagation of a wave packet localized in a narrow frequency band.[22,23] A series of such wave packets can approximate the evolution of the broad spectrum disturbances to some degree of accuracy. This explains why an isolated wave packet is one of the most popular subjects of inquiry in the boundary layer stability problem.[24-26]
In Section 2, we formulate the problem. In Section 3, we discuss DNS of two-dimensional wave packet propagatiing in the boundary layer over a flat plate at the free-stream Mach number 6. An isolated wave packet is initialized by a localized in space and time blowing-suction as well as by fast and slow acoustic waves of zero angle of incidence. The wave packet, which is excited in the boundary layer, contains different modes. Each mode amplifies or decays during the wave-packet propagation. Ultimately, the overall motion will consist of the sum of these modes suitably weighted, in both phase and growth, by factors appropriate to the dispersion law.
We also consider a separating flow over a compression corner (Section 4) at the freestream Mach number $\mathrm{M}_\infty = 5.373$. This configuration is typical for various units of high-speed vehicles: ducted air intake surface breaks, generating oblique shock waves, deflected steering surfaces (such as balancing flaps) *etc*. Typically the near-wall flow over a supersonic compression corner comprises: the boundary layer upstream separation, the shear layer and recirculating flow in the separation bubble, the reattached boundary layer. Details of the wave-packet propagation through these regions are discussed. The paper is concluded in Section 5.

2. Problem formulation

Viscous two-dimensional unsteady compressible flows are governed by the Navier-Stokes equations resulting from conservation laws of mass, momentum and energy. The fluid is a perfect gas of the specific heat ratio $\gamma = 1.4$ and Prandtl number $\mathrm{Pr} = 0.72$. The viscosity-temperature dependence is approximated by the power law $\mu^* / \mu_\infty^* = \left(T^* / T_\infty^*\right)^{0.7}$. Calculations are carried out for hypersonic flow over a flat plate with sharp leading edge at the freestream Mach number $\mathrm{M}_\infty = 6$ and Reynolds number $\mathrm{Re}_\infty = \rho_\infty^* U_\infty^* L^* / \mu_\infty^* = 2\times10^6$. Hereafter ρ_∞^* is freestream density, U_∞^* is freestream velocity, L^* is plate length, asterisks denote dimensional quantities. The flow variables are made nondimensional using undisturbed freestream parameters: $(u,v) = (u^*, v^*)/U_\infty^*$ – velocity components, $p = p^* /(\rho_\infty^* u_\infty^{*2})$ – pressure, $\rho = \rho / \rho_\infty^*$ – density, $T = T^* / T_\infty^*$ – temperature. Dimensionless coordinates and time are $(x, y) = (x^*, y^*)/L^*$, $t = t^* U_\infty^* / L^*$.
The boundary conditions on the solid wall ($y = 0$) are: no-slip condition $(u,v) = 0$; $\partial T_w / \partial y = 0$ corresponding to the adiabatic wall. On the outflow boundary, the unknown variables u, v, p, T are extrapolated using linear approximation. On the inflow and upper boundaries, conditions correspond to the undisturbed free stream. Details on the problem formulation and governing equations are given in Ref. 20.
The problem is solved numerically using the implicit second-order finite-volume method.[20] Two-dimensional Navier-Stokes equations are approximated by TVD shock-capturing scheme. It allows for modeling of the disturbance dynamics in the leading-edge vicinity, where receptivity to free-stream disturbances is most pronounced. Nevertheless this computational scheme damps physical waves, especially near the peaks and valleys. The numerical dissipation can be suppressed using sufficiently fine computational grids. Egorov et al.[20] carried out 2-D DNS of disturbances generated by a local periodic suction-blowing in the boundary layer on a flat plate at the freestream parameters considered herein. It was shown that the grid of 1501×201 nodes (with clustering in the boundary layer and leading-edge region) is appropriate for modeling of the boundary-layer instability. Namely, the calculated second-mode growth rate agreed well with that predicted by LST. With this reasoning the aforementioned computational grid is used for 2-D DNS discussed hereafter.
At first, the steady-state solution, which satisfies the undisturbed free-stream boundary conditions on the inflow and upper boundaries, is calculated to provide the mean laminar flow. The steady pressure field (figure 1) indicates that the viscous-inviscid interaction of the boundary layer with the free stream leads to formation of a shock wave emanating from the plate leading edge.

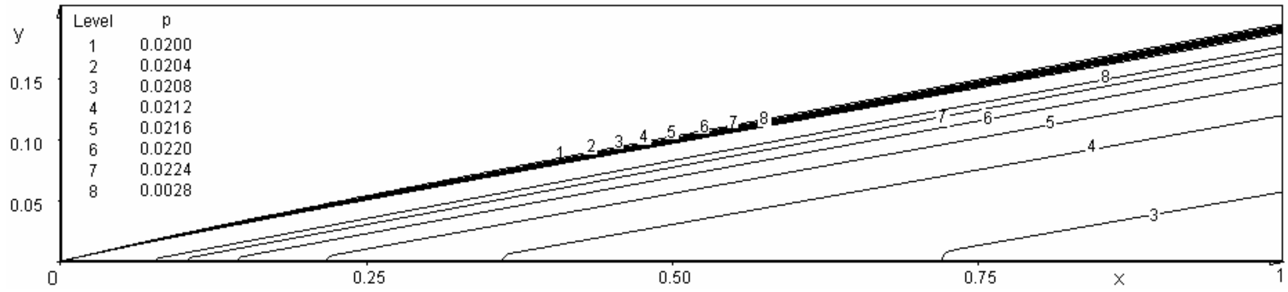

Figure 1: Pressure contours in the computational domain

3. Wave packet evolution in the boundary layer over flat plate

3.1 Disturbances induced by suction-blowing

For investigation of the boundary-layer stability, the initial disturbances are induced by the boundary condition that models a local periodic suction-blowing near the leading edge. The mass flow on the plate surface is given by

$$q_w(x,t) = \frac{\rho_w^* v_w^*}{\rho_\infty^* U_\infty^*} = \varepsilon \sin\left(2\pi \frac{x-x_1}{x_2-x_1}\right)\sin(\omega t),\ \ x_1 \le x \le x_2,\ 0 \le t \le nT\,, \quad \textbf{(1)}$$

where ε is forcing amplitude; $x_1 = 0.0358$, $x_2 = 0.0495$ are boundaries of the suction-blowing region; the circular frequency $\omega = \omega^* L^* / U_\infty^* = 260$ corresponds to the frequency parameter $F = \omega / \mathrm{Re}_\infty = 1.3\times10^{-4}$; $T = 2\pi/\omega$ is time period; n is number of wavelengths of initial wave packet. The initial wave packets contain one wavelength ($n=1$, a short packet) or four wave lengths ($n=4$, a long packet). The suction-blowing amplitude is $\varepsilon = 1\times10^{-3}$, at which disturbance evolution is linear. For the unsteady problem, the wall temperature corresponds to the adiabatic wall, $T_w(x,t) = T_{ad}(x)$; i.e., the temperature disturbance is zero on the plate surface. The difference between the instantaneous flow field and the steady-state flow field represents the disturbance field.
The pressure disturbances on the plate surface are shown in figure 2 at fixed time moments for the cases of short, long wave packets and in the case of source acting infinitely long time ($n=\infty$). The amplitude of the long wave-packet is close enough to the amplitude of disturbances induced by a permanently acting source, while the amplitude of the short wave-packet is distant from these disturbances.
For simulation of nonlinear effects, the forcing amplitude was increased to the level $\varepsilon = 3.6\times10^{-2}$. Comparison of the wave-packet amplitudes on the wall surface is shown in figure 3 at the time moment $t=1$. As one can see, the nonlinear wave-packet has a different phase characteristics.

3.2 Disturbances induced by fast and slow acoustic waves

For modelling of receptivity to acoustic disturbances, a plain monochromatic acoustic wave is imposed on the free stream as

$$(u',v',p',T')_\infty^T = (|u'|,|v'|,|p'|,|T'|)_\infty^T \exp\left[i(k_\infty x - \omega t)\right],\ \ 0 \le t \le nT\,,$$

where $|u'|$, $|v'|$, $|p'|$, $|T'|$ are dimensionless amplitudes

$$|u'| = \pm \mathrm{M}_\infty |p'|,\ |v'| = 0,\ |p'| = \varepsilon,\ |T'| = (\gamma-1)\mathrm{M}_\infty^2 |p'|$$

the upper (lower) sign corresponds to the fast (slow) acoustic wave. The wavenumber is expressed as $k_\infty = \omega M_\infty / (M_\infty \pm 1)$. Herein we consider acoustic waves of small amplitude $\varepsilon = 5\times10^{-5}$ at which the receptivity process is linear. The disturbance frequency $\omega = 260$. The initial disturbance contains four wave-length (long wave packet of $n = 4$).

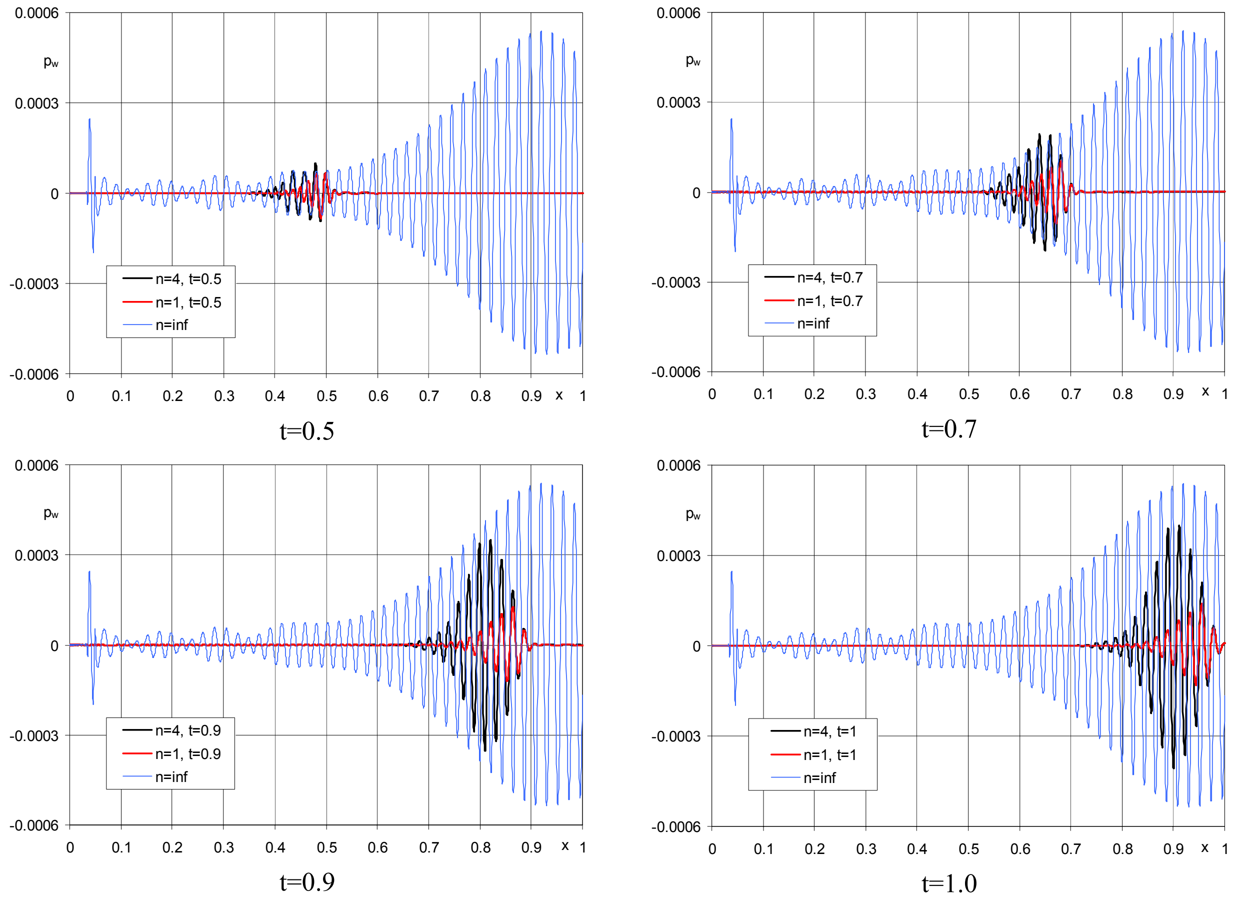

Figure 2: Pressure disturbance amplitudes for the linear case; black line – long wave packet, red line – short wave packet, blue line – permanently acting source

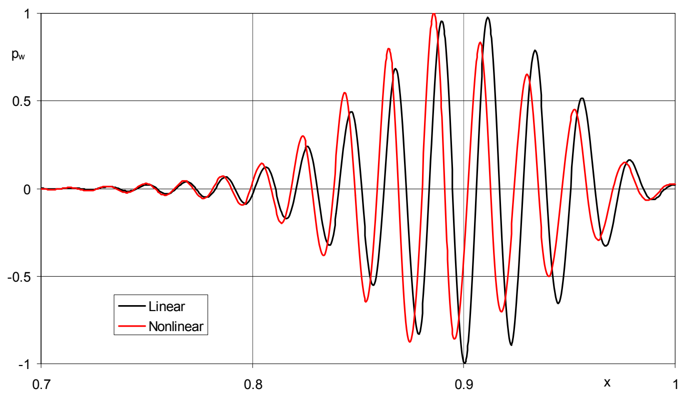

Figure 3: Wall pressure disturbance amplitudes for the linear (black line) and nonlinear (red line) cases

Receptivity to free-stream disturbances depends on both the level of acoustic near field (which results from the interaction between the incident disturbance and the leading-edge shock wave) and the difference between phase speeds of unstable boundary-layer waves and incident acoustic disturbances (synchronization condition). Details of the numerical simulation of receptivity to permanently acting free-stream acoustic disturbances at different angles of incidence are given in Ref. 21.

The wall pressure disturbances induced by the long wave-packet of fast and slow incident acoustic wave are shown in figure 4. Receptivity to slow acoustic waves is essentially higher than that to fast waves. The pressure fields in the case of fast wave are shown in figure 5 at different time moments. The pressure amplitude is relatively small in a layer, which occurs just above the boundary layer. This "quiet" layer separates the external acoustic field from the boundary-layer disturbances in a way that is consistent with the theoretical prediction[10] for acoustic disturbances in the diffraction zone. The external acoustic field propagates downstream with the phase speed of fast acoustic wave 1+1/M. The wave packet in the boundary layer travels downstream with relatively slow speed. As the wave packet evolves downstream, it disperses in space.

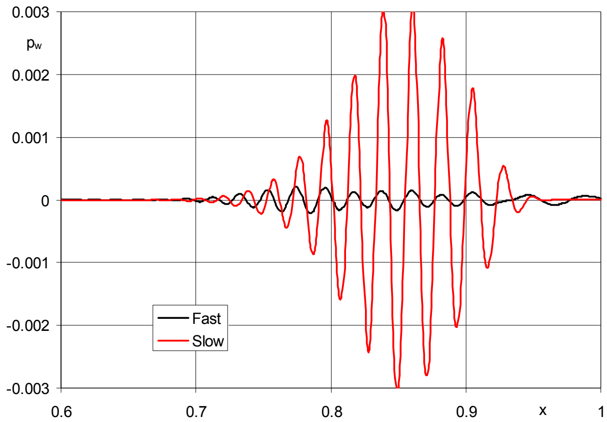

Figure 4: Wall pressure disturbance amplitudes for the case of fast (black line) and slow (red line) incident acoustic wave, $t = 1$

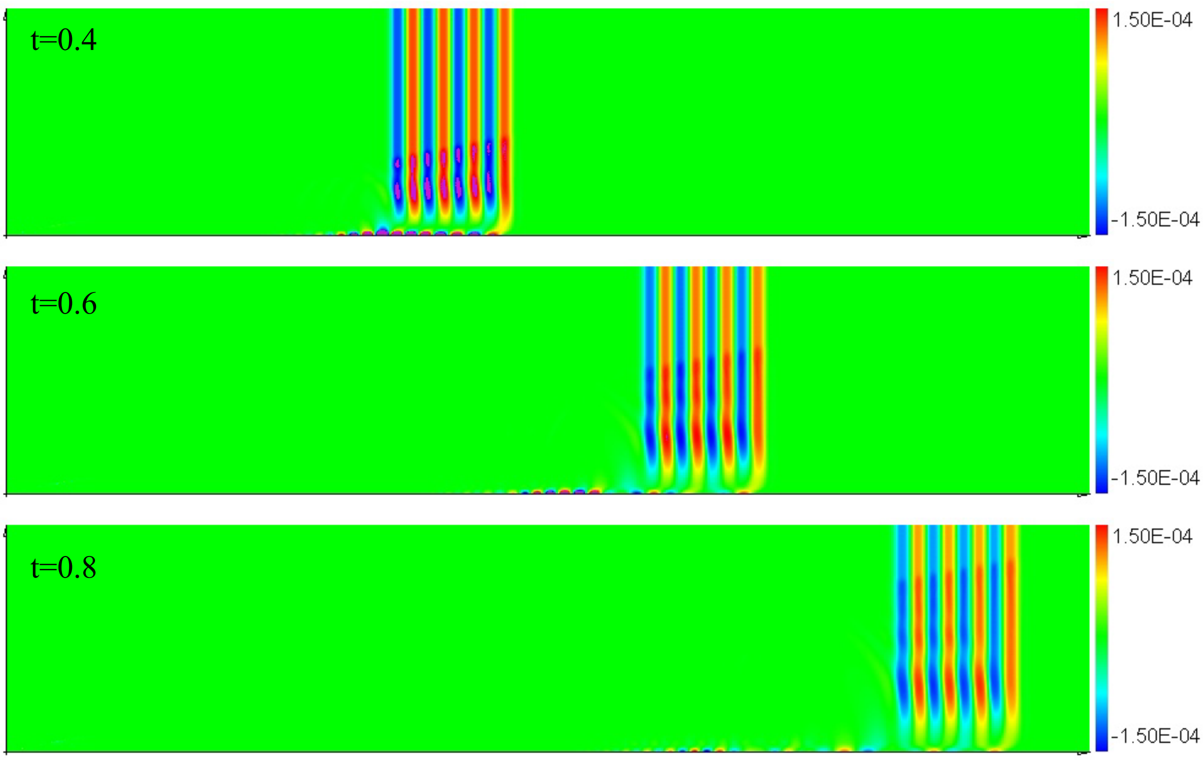

Figure 5: Pressure fields for the case of fast acoustic wave

4. Wave packet evolution in the boundary layer over compression corner

Consider flow over a compression corner[17] with the inclination angle $\alpha = 5.5^\circ$. Flow variables are made nondimensional using the same quantities as in the flat-plate case with L^* being a distance from the leading edge to the corner point. Calculations are carried out for the flow parameters: $\mathrm{M}_\infty = 5.373$, $\mathrm{Re}_\infty = 5.667 \times 10^6$, $\gamma = 1.4$, $\mathrm{Pr} = 0.72$, $T_\infty^* = 74.194\,\mathrm{K}$. The wall temperature is $T_w = 4.043$ ($T_w^* = 300\,\mathrm{K}$). Dynamic viscosity

μ is approximated using the Sutherland formula. The computational grid has 2801×221 nodes. The grid nodes were clustered in the boundary-layer and leading-edge regions. No-slip boundary conditions are imposed on the bottom surface.

Because of the viscous-inviscid interaction, a shock wave forms in the leading edge vicinity. In the corner region, there are compression waves that interact with the boundary layer and induce a recirculation zone (separation bubble). The upper boundary of this zone is approximately a straight line that is typical for supersonic separation. Downstream from the reattachment point, the boundary layer is thinner than in the upstream vicinity of separation point.

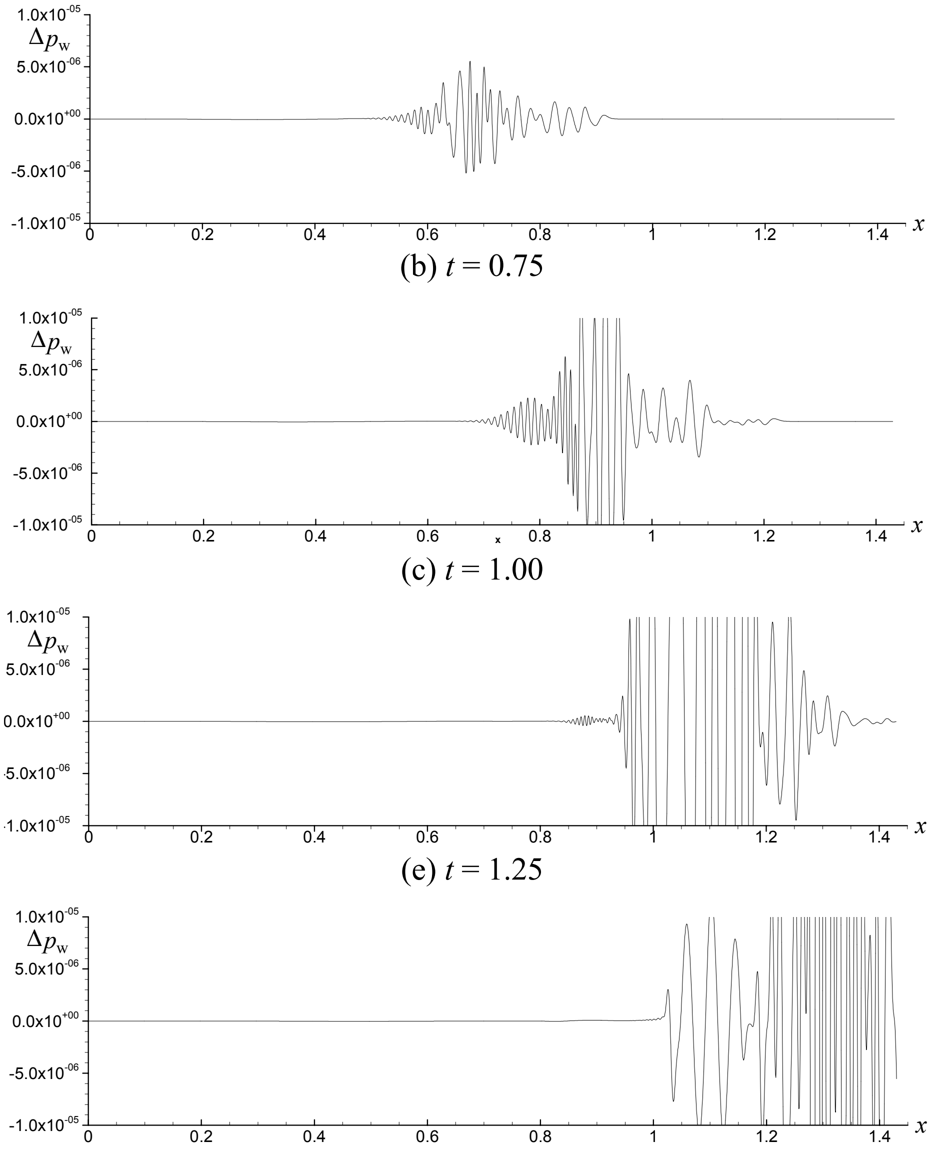

Figure 6: Wall pressure disturbances for the case of wave packet over the compression corner

A local suction-blowing is introduced into the flow using the boundary condition (1) on the plate surface with $\varepsilon = 10^{-3}$, $x_1 = 0.0358$, $x_2 = 0.0521$ and $\omega = 450$, $n = 5$.

While the wave packet propagates through the separation zone, a sharp growth of the disturbance amplitude is observed in the numerical solution. This behaviour is essentially different from the case of the wave-packet evolution in the boundary layer over a flat plate. Moreover, such a sharp growth is not observed in the case of permanently acting source. This effect probably is due to the relatively broad spectrum of the wave packet and the presence of several length scales in the separation bubble. The wall pressure disturbances generated by blowing-suction are shown in figure 6 in the corner region at different time moments.

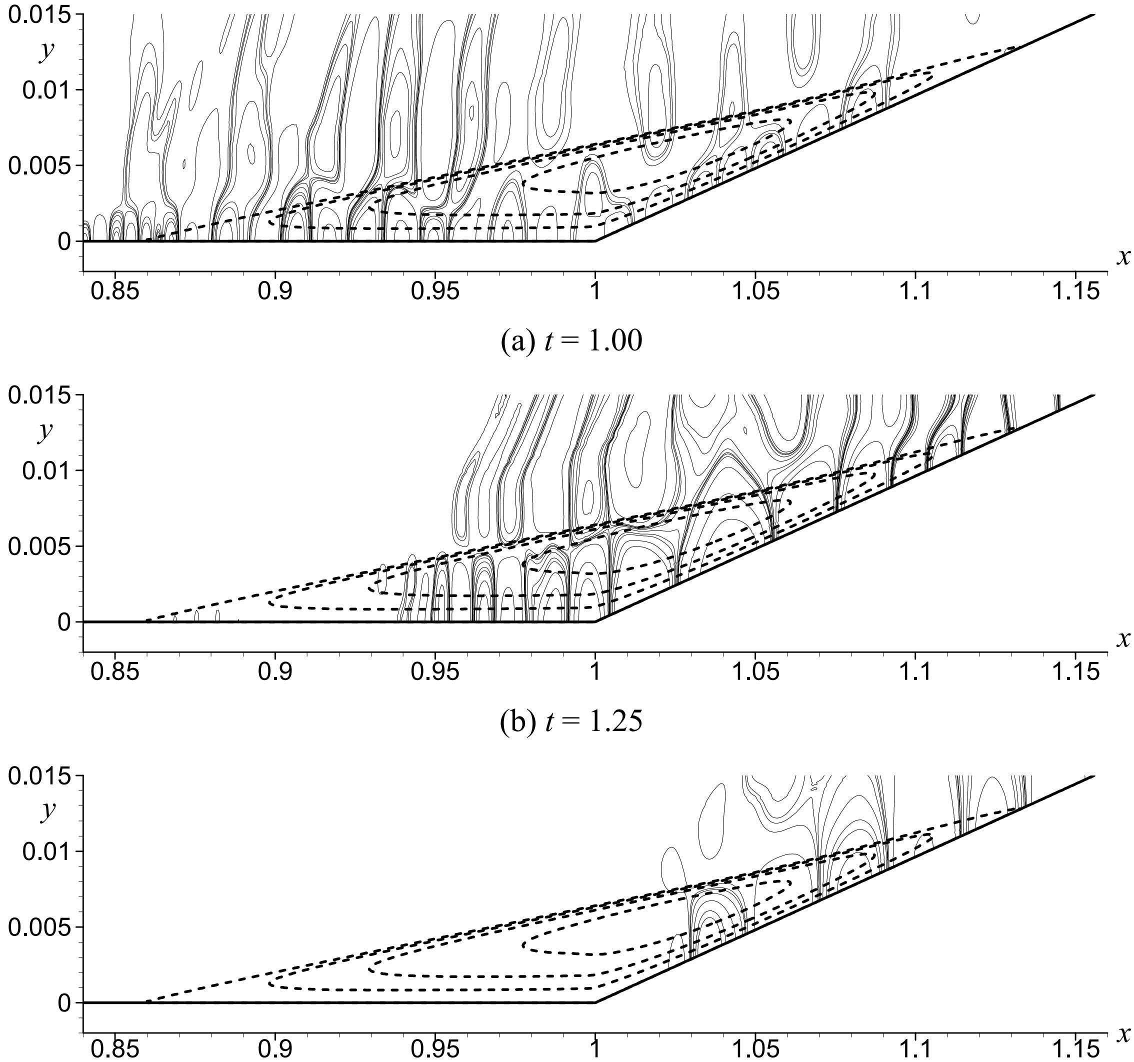

(a) t = 1.00

(b) t = 1.25

(c) t = 1.50

Figure 7: Pressure disturbance contours for in the separation bubble of compression corner, dashed lines denote streamlines of the mean flow

5. Conclusions

Two-dimensional direct numerical simulation of the wave-packet evolution in a supersonic boundary layer over a flat plate was carried out. Excitation of wave-packets in the boundary layer by blowing-suction, fast and slow acoustic waves was considered. The amplitude of the long wave-packet induced by blowing-suction is close to the amplitude of disturbances induced by a permanently acting source, while the amplitude of short wave-packet is distant from these disturbances. In the nonlinear case, dispersion characteristics of the wave packet are different from that observed in the linear case.

Receptivity to free-stream disturbances depends on both the level of acoustic near field (that is associated with the interaction between the incident disturbances and the leading-edge shock wave) and the difference between phase speeds of unstable boundary-layer waves and incident acoustic disturbances (that is associated with the synchronization condition). Receptivity to slow acoustic waves is essentially higher than that to fast waves.

As the wave packet propagates through the separation zone in the compression corner, a sharp growth of the disturbance amplitude is observed in the numerical solution. This behaviour is essentially different from the case of wave-packet evolution in the boundary layer over a flat plate. Such a growth is not observed in the case of permanently acting source. Presumably, this effect is due to the relatively broad spectrum of the wave packet and the presence of several length scales in the separation bubble.

This work was supported financially by the Russian Foundation for Basic Research (Grants No 06-08-01214, 05-01-00562) and performed under the contract to the International Science and Technology Center (ISTC), Moscow.

References

[1] Morkovin M.V. Critical evaluation of transition from laminar to turbulent shear layers with emphasis on hypersonic traveling bodies. AFRL Report AFFDL-TR-68-149. Air Force Flight Dynamics Laboratory, Wright-Patterson AFB, OH, USA, 1969.
[2] Malik M., Zang T. and Bushnell D. Boundary Layer Transition in Hypersonic Flows. *AIAA Paper* 90-5232.
[3] Reshotko E. Boundary-layer stability and transition. *Ann. Rev. Fluid Mech.* 8:311-349, 1976.
[4] Mack L.M. Boundary layer stability theory. Part B. Doc. 900-277, JPL, Pasadena, California, May, 1969.
[5] Demetriades A. Hypersonic viscous flow over a slender cone, part III: Laminar instability and transition. *AIAA Paper* 74-535.
[6] Kendall J.M. Wind tunnel experiments relating to supersonic and hypersonic boundary layer transition. *AIAA J.* 13:290-299, 1975.
[7] Stetson K.F., Kimmel R., Thompson E.R., Donaldson J.C. and Siler L.G. A comparison of a planar and conical boundary layer stability and transition at Mach number of 8. *AIAA Paper* 91-1639.
[8] Mack L.M. Boundary-layer stability theory. Special course on stability and transition of laminar flow (ed. R. Michel), AGARD Rep. 709, pp. 3-1–3-81, 1984.
[9] Guschin V.R. and Fedorov A.V. Short-wave instability in a perfect-gas shock layer. *Fluid Dynamics,* 24(1):7-10, 1989.
[10] Fedorov A.V. and Khokhlov A.P. Excitation of unstable modes in supersonic boundary layer by acoustic waves. *Fluid Dynamics,* 9:456-467, 1991.
[11] Fedorov A.V. Receptivity of a high-speed boundary layer to acoustic disturbances. *J. Fluid Mech.* 491:101-129, 2003.
[12] Maslov A.A., Shiplyuk A.N., Sidorenko A. and Arnal D. Leading-edge receptivity of a hypersonic boundary layer on a flat plate. *J. Fluid Mech*. 426:73-94, 2001.
[13] Ma Y. and Zhong X. Numerical simulation of receptivity and stability of nonequilibrium reacting hypersonic boundary layers. *AIAA Paper* 2001-0892.
[14] Zhong X. Leading-edge receptivity to free-stream disturbance waves for hypersonic flow over parabola. *J. Fluid. Mech.* 441:315-367, 2001.
[15] Ma Y. and Zhong X. Receptivity of a supersonic boundary layer over a flat plate. Part 1. Wave structures and interactions. *J. Fluid. Mech*. 488:31-78, 2003.
[16] Ma Y. and Zhong X. Receptivity of a supersonic boundary layer over a flat plate. Part 2. Receptivity to free-stream sound. *J. Fluid. Mech*. 488:79-121, 2003.
[17] Balakumar P., Zhao H. and Atkins H. Stability of hypersonic boundary-layer over a compression corner. *AIAA Paper* 2002-2848.
[18] Malik M.R. and Balakumar P. Receptivity of Supersonic Boundary Layers to Acoustic Disturbances. *AIAA Paper* 2005-5027.
[19] Kara K., Balakumar P. and Kandil O.A. Receptivity of Hypersonic Boundary Layers Due to Acoustic Disturbances over Blunt Cone. *AIAA Paper* 2007-945.
[20] Egorov I.V., Fedorov A.V. and Soudakov V.G. Direct numerical simulation of disturbances generated by periodic suction-blowing in a hypersonic boundary layer. *Theoret. Comput. Fluid Dynamics*, 20(1):41-54, 2006.
[21] Egorov I.V., Fedorov A.V. and Soudakov V.G. Direct numerical simulation of supersonic boundary layer receptivity to acoustic disturbances. *AIAA Paper* 2005-97.
[22] Gaster M. The development of three-dimensional wave packets in a boundary layer. . *Fluid. Mech*. 32:173-184, 1968.
[23] Gaster M. Propagation of linear wave packets in laminar boundary layers. *AIAA J*. 19(4):419-423, 1981.
[24] Nayfeh A.H. Stability of three-dimensional boundary layers. *AIAA J.* 18(4):406-416, 1980.
[25] Zelman M.B., Smorodsky B.V. On wave disturbances packets of Blasius flow. *Fluid Dynamics,* 1:32-38, 1988
[26] Forgoston E., Tumin A. Three-dimensional wave packet in a hypersonic boundary layer. *AIAA Paper* 2005-99.

This page has been purposedly left blank